OXFORD

High-definition transcranial direct current stimulation enhances network segregation during spatial navigation in mild cognitive impairment

Alexandru D. Iordan [ID]^1,2, Shannon Ryan [ID]^2, Troy Tyszkowski [ID]^2, Scott J. Peltier [ID]^3,4, Annalise Rahman-Filipiak [ID]^2,

Benjamin M. Hampstead [ID]^2,5,*

[1]Department of Psychology, University of Michigan, Ann Arbor, MI 48109, USA,
[2]Research Program on Cognition and Neuromodulation Based Interventions, Department of Psychiatry, University of Michigan, Ann Arbor, MI 48105, USA,
[3]Functional MRI Laboratory, University of Michigan, Ann Arbor, MI 48109, USA,
[4]Department of Biomedical Engineering, University of Michigan, Ann Arbor, MI 48109, USA,
[5]VA Ann Arbor Healthcare System, Neuropsychology Section, Mental Health Service, Ann Arbor, MI 48105, USA
*Corresponding author: University of Michigan, 2101 Commonwealth Blvd Ste C, Ann Arbor, MI 48105, USA. Email: bhampste@med.umich.edu

Spatial navigation is essential for everyday life and relies on complex network-level interactions. Recent evidence suggests that transcranial direct current stimulation (tDCS) can influence the activity of large-scale functional brain networks. We characterized brain-wide changes in functional network segregation (i.e. the balance of within- vs. between-network connectivity strength) induced by high-definition (HD) tDCS in older adults with mild cognitive impairment (MCI) during virtual spatial navigation. Twenty patients with MCI and 22 cognitively intact older adults (healthy controls—HC) underwent functional magnetic resonance imaging following two counterbalanced HD-tDCS sessions (one active, one sham) that targeted the right parietal cortex (center anode at P2) and delivered 2 mA for 20 min. Compared to HC, MCI patients showed lower brain-wide network segregation following sham HD-tDCS. However, following active HD-tDCS, MCI patients' network segregation increased to levels similar to those in HC, suggesting functional normalization. Follow-up analyses indicated that the increase in network segregation for MCI patients was driven by HD-tDCS effects on the "high-level"/association brain networks, in particular the dorsal-attention and default-mode networks. HD-tDCS over the right parietal cortex may normalize the segregation/integration balance of association networks during spatial navigation in MCI patients, highlighting its potential to restore brain activity in Alzheimer's disease.

Key words: aging; functional connectivity; neuromodulation; restoration; transcranial electrical stimulation..

Introduction

Spatial navigation is essential for everyday life and involves both allocentric and egocentric strategies. Whereas allocentric navigation uses external references (i.e. landmarks) and relies mainly on medial temporal and parietal brain regions, egocentric navigation uses an internal reference system, and engages the striatum, especially the caudate nucleus (Boccia et al. 2014). Although specific neural mechanisms may be preferentially recruited for implementing individual spatial functions, navigation, like all complex behaviors, is a brain-wide network phenomenon (Brunyé 2017; Ekstrom et al. 2017; Cona and Scarpazza 2019).

Among the multiple brain regions supporting navigation, a core frontoparietal network—comprising the superior parietal lobule (extending into the intraparietal sulcus laterally and precuneus medially), dorsal premotor regions, and frontal eye fields (junction of the superior frontal sulcus and precentral sulcus)—is generally identified across spatial navigation tasks

(Cona and Scarpazza 2019). This dorsal-attention network plays a key role in visuospatial attention and is thought to implement higher order representation (or "prioritization") of behaviorally relevant spatial locations (Corbetta and Shulman 2002; Petersen and Posner 2012; Jerde and Curtis 2013).

In addition, two other large-scale networks are often discussed in relation to the dorsal-attention network and its function. First, the default-mode network, anchored in the medial prefrontal and posterior cingulate cortices, has been implicated in self-referential processing, mentalizing, and episodic memory (Raichle et al. 2001; Greicius et al. 2003; Buckner et al. 2008), which are all relevant for learning and recalling knowledge of the environment one is to navigate (Smallwood et al. 2021). While the dorsal-attention and default-mode networks are often thought to implement competing modes of processing—due to their preferential orientation toward external and internal environments, respectively (Fox et al. 2005; Dixon et al. 2017)—they are both vital

to successful navigation, since attending to external cues interacts with internally based knowledge of the environment. Second, the frontoparietal control network, anchored in the dorsolateral prefrontal and lateral parietal cortices, plays a central role in moment-to-moment cognitive control (Dosenbach et al. 2007; Duncan 2010; Power and Petersen 2013). The frontoparietal control network is extensively interconnected with both the dorsal-attention and default-mode networks, and is thought to dynamically modulate the activity of those networks as a function of task goals and demands (Spreng et al. 2013; Dixon et al. 2018).

Cognitive performance critically depends on the brain's ability to recruit neural circuits specialized for the execution of the task at hand (Dehaene et al. 1998). This ability is supported by the brain's functional organization into distinguishable networks that show greater within- than between-network connectivity, that is are segregated from each-other (Crossley et al. 2013). Network segregation typically decreases with "normal" aging and is further impacted by neurodegenerative diseases like Alzheimer's disease (AD) (Brier et al. 2014; Damoiseaux 2017) and its clinical precursor, mild cognitive impairment (MCI) (Petersen 2001; Petersen et al. 2009). One explanation for such declines is neural dedifferentiation, a process by which neural networks lose their distinctiveness, leading to (over)recruitment of network ensembles instead of individual components responsible for specialized operations (Park et al. 2004; Grady 2012). Furthermore, "associative" brain networks that mediate higher-level functions (such as the dorsal-attention, frontoparietal, and default-mode networks) are disproportionately affected by both "normal" aging and further in those with MCI, compared to preserved "sensory-motor" networks (such as the somato-sensorimotor and visual networks) (Chan et al. 2014; Geerligs et al. 2015; Iordan et al. 2018).

Transcranial direct current stimulation (tDCS) is a promising noninvasive, nonpharmacological intervention for AD and related dementias (Meinzer et al. 2015). Accumulating evidence shows that local tDCS can influence brain-network activity both during task performance and at rest, suggesting that stimulation acts at the level of functional networks rather than isolated brain regions (Keeser et al. 2011; Polanía et al. 2011; Peña-Gómez et al. 2012; Sehm et al. 2013; Li et al. 2019); see also (Sale et al. 2015; To et al. 2018) for recent reviews. However, few investigations have evaluated the effects of tDCS on spatial navigation. We are aware of only one previous study that examined the effects of tDCS over the parietal cortex, which was performed in healthy younger adults and identified modulation of a network comprising prefrontal, parietal, and subcortical (i.e. caudate) regions, during both virtual navigation (Hampstead et al. 2014) and the resting-state (Krishnamurthy et al. 2015). Thus, it is currently unknown *if* and *how* tDCS influences large-scale network

function in older adults with and without cognitive impairments.

Here, we report the results of a double blind, crossover, randomized controlled trial that examined the effects of tDCS over the right superior parietal cortex on allocentric and egocentric navigation in cognitively intact older adults and in individuals with MCI due to presumed AD. We employed high-definition (HD) tDCS, which provides more focal stimulation than conventional tDCS (Cano et al. 2013) and has not been previously employed in navigation studies. In addition, we targeted the right parietal cortex in an attempt to enhance the spatial aspects of cognitive processing (Cona and Scarpazza 2019). As an extension of our previous work (Hampstead et al. 2014; Krishnamurthy et al. 2015), we employed a validated virtual navigation task in conjunction with task-related and resting-state functional magnetic resonance imaging (fMRI) recordings, which were collected following both active and sham HD-tDCS. Our main outcome measure was *network segregation*, a recently proposed index of functional network specificity or distinctiveness.

Based on previous evidence (e.g. Brier et al. 2014), we expected that sham HD-tDCS would be more reflective of an actual baseline where those with MCI show lower network segregation compared to HC. We also expected that HD-tDCS over the right superior parietal cortex would increase engagement of that brain region and result in increased network segregation. That is, if HD-tDCS normalizes network recruitment, then it would enhance the engagement of task-relevant networks, thus strengthening their segregation, potentially similar to effects reported for cognitive training (Lebedev et al. 2018). However, it remains an open question whether this effect would be evident for both controls and MCI patients. We envisioned three possibilities: (1) if segregation increased in both groups, then it would suggest HD-tDCS effects regardless of clinical phenotype; (2) if segregation increased for controls but not for MCI patients, then it would suggest that the presumed disease process is not responsive to HD-tDCS; (3) if segregation increased for MCI patients but not for controls, then it would suggest restorative effects in MCI, while the absence of change in controls could reflect relative integrity of the system and raise questions about dose–response relationships. Finally, regarding segregation of individual networks, we expected HD-tDCS effects particularly at the level of task-relevant association networks that include the lateral parietal cortex as a major "hub," such as the dorsal-attention, default-mode, and frontoparietal networks.

Materials and methods
Participants

Forty-two, right-handed and MRI-compatible older adults completed this clinical trial (NCT01958437). Participant diagnosis was achieved via a consensus

Table 1. Demographic, neuropsychological, and EF characteristics of the HC and MCI groups.

Demographic/Measure			HC Group (n = 22) M (SD)	MCI Group (n = 20) M (SD)	Group differences
Age			69.50 (6.55)	72.15 (7.14)	$t = 1.25, P = 0.217$
Sex			10 m/12f	13 m/7f	$\chi^2 = 1.62, P = 0.204$
Education (years)			15.68 (2.12)	16.65 (2.6)	$t = 1.33, P = 0.19$
MoCA (raw score)			26 (2.53)	23.65 (3.33)	$t = 2.59, P = 0.13$
WTAR (word reading)			114 (9.62)	108.6 (12.64)	$t = 1.57, P = 0.125$
RBANS immediate memory			99.55 (15.71)	77.95 (11.3)	$t = 5.07, P < 0.001***$
RBANS visuospatial			111.32 (13.32)	102.4 (17.14)	$t = 1.89, P = 0.066$
RBANS language			104.09 (9.86)	94.65 (9.47)	$t = 3.16, P = 0.003**$
RBANS attention			110.32 (17.49)	102.3 (12.67)	$t = 1.69, P = 0.1$
RBANS delayed memory			103.64 (12.44)	72.74 (19.74)	$t = 5.89, P < 0.001***$
Trails A (z-score)			0.71 (0.9)	0.16 (0.96)	$t = 1.49, P = 0.145$
Trails B (z-score)			0.76 (0.99)	0.23 (1.31)	$t = 2.59, P = 0.013*$
Electric field P2 ROI (V/m)			0.14 (0.05)	0.13 (0.03)	$t = 0.44, P = 0.66$
Residual head motion (mean displacement)					
	Task				
		Active	0.19 (0.1)	0.2 (0.09)	$t = 0.4, P = 0.692$
		Sham	0.2 (0.1)	0.19 (0.1)	$t = 0.3, P = 0.767$
	Rest				
		Active	0.14 (0.07)	0.16 (0.08)	$t = 0.9, P = 0.374$
		Sham	0.15 (0.08)	0.14 (0.06)	$t = 0.49, P = 0.626$
Amount of data retained (scans)					
	Task				
		Active	1197.59 (21.79)	1191.7 (25.29)	$t = 0.81, P = 0.422$
		Sham	1197.86 (18.3)	1187.7 (27.2)	$t = 1.43, P = 0.16$
	Rest				
		Active	502.91 (4.45)	500.85 (7.18)	$t = 1.13, P = 0.266$
		Sham	500.36 (11.15)	500.45 (9.23)	$t = 0.03, P = 0.978$

All test scores represent standard scores (M = 100, SD = 15), unless otherwise specified. Abbreviations: m, male; f, female; MoCA, Montreal Cognitive Assessment; WTAR, Wechsler Test of Adult Reading; RBANS, Repeatable Battery for the Assessment of Neuropsychological Status; ROI, region of interest.

diagnosis in which all relevant data were considered (e.g. neurological examination, neuropsychological testing, neuroimaging). Twenty participants were diagnosed with amnestic MCI with a presumed AD etiology, following the Albert et al. (2011) criteria (i.e. subjective complaint, objective evidence of impairment, but intact everyday functioning). Twenty-two older adults were deemed to be cognitively unimpaired and are referred to as healthy controls (HC) hereafter. There were no between-group differences on demographic variables (Table 1). Exclusion criteria included history of other contributing neurological (i.e. epilepsy, moderate–severe traumatic brain injury) or medical conditions known to affect cognitive functioning, significant mental illness (e.g. moderate to severe depression, bipolar disorder, schizophrenia), sensory impairments that limited their ability to participate in the study, or a history of alcohol or drug abuse/dependence. The Veterans Affairs Ann Arbor Healthcare System's (VA AAHS) Institutional Research Board approved this study. All participants provided written informed consent. Any protocol amendment were approved by the VA AAHS and necessary modifications made to https://clinicaltrials.gov.

Procedures

Following written informed consent, participants underwent a brief neuropsychological protocol (Table 1). Eligible participants were randomized to receive sham HD-tDCS followed by active, or the opposite order, using the sealed envelope method. Specifically, the tDCS clinical trial units were preprogrammed with 6-digit codes that enabled the unit to provide either active or sham stimulation. One active and one sham code were included in each envelope (all codes were unique for each session and participant), in a specified order (i.e. active→sham or sham→active) prior to the start of the study. These envelopes were then sealed, shuffled, and numbered. At the start of the first session, study team members would take the next envelope, open it, and enter the session-appropriate code. This ensured that both study team member and participant were blind to the stimulation condition. These codes were maintained in the participant files until enrollment and all data collection were complete, at which point the blind was broken (i.e. each code was identified as either active or sham).

The structure of each session (i.e. sham or active HD-tDCS) was identical as both started with HD-tDCS and then proceeded to MRI scanning. At least 48 h separated tDCS sessions 1 and 2 (Fig. 1a) since motor physiology suggests single-session tDCS effects dissipate within minutes to hours (Kuo et al. 2013). Supplementary analyses showed that the number of days [M (SD) 7.79 (6.93) days] between the first and the second session had no effect on performance in the navigation tasks (see Supplementary Results).
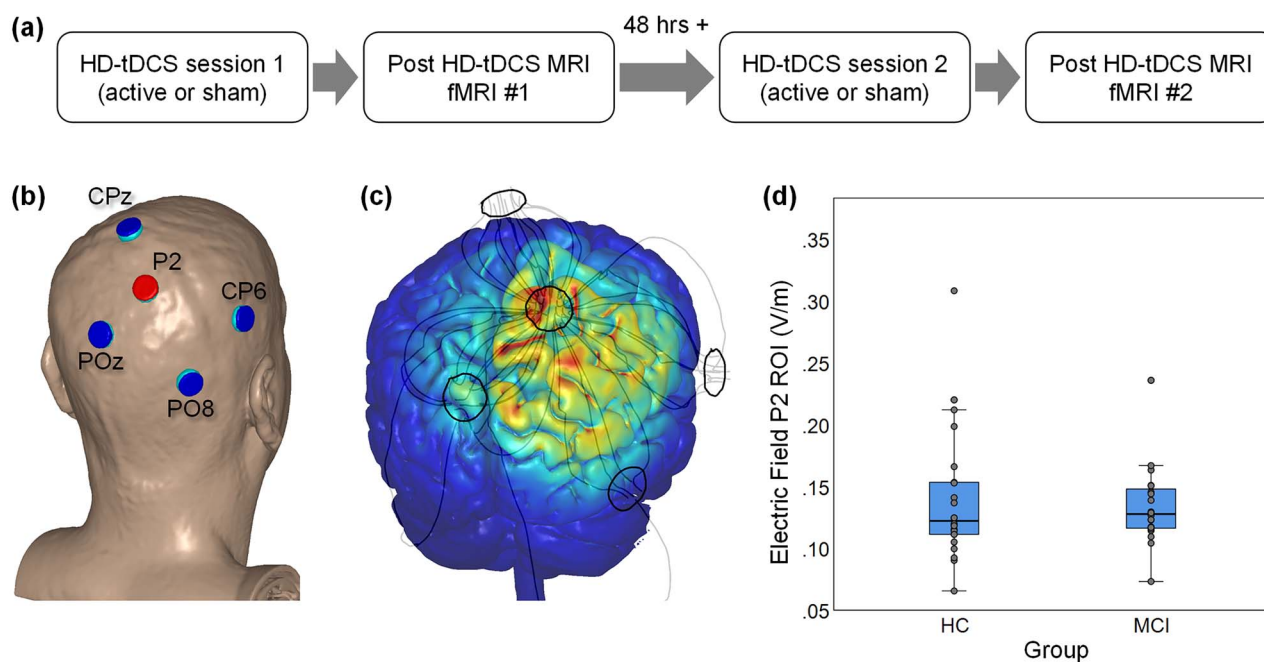
Fig. 1. Experimental design, electrode locations, and EF. (a) Diagram of the experimental design. (b) Electrode placement using a model head (center anode shown in red; surrounding cathodes shown in blue). (c) Finite-element model of the EF using a model brain. (d) Actual EF values extracted from the P2 ROI for HC and patients with MCI. Each box displays the median (horizontal line), 25th and 75th percentiles (bottom and top box edges), 1.5 times the interquartile range (whiskers), and observed values for each individual (gray circles).

Navigation task

We updated our virtual navigation task (Hampstead et al. 2014; Krishnamurthy et al. 2015) based on experience from the earlier study using MazeSuite 2.0 (www. mazesuite.com) or Plan3D (www.plan3d.com) to create the virtual environments. Nine allocentric environments (e.g. house, shopping center) included multiple landmarks or distinguishing features (e.g. rooms of a house). We intentionally constructed the fMRI task and associated instructions to bias cognitive processing toward either allocentric or egocentric processing. Specifically, videos showed unique paths through each allocentric environment. Participants were instructed to ignore the series of turns and attend to the specific landmarks (or key details) and create a mental map that integrated the spatial relationships of these landmarks to one another. In contrast, a single path was recorded through each of the 9 egocentric environments. Participants were instructed to focus on the series of left/right turns, remembering them in order. They were explicitly told not to create a mental map of these environments since they all used the same general layout and only the series of turns differed between them.

The fMRI paradigm consisted of 3 functional runs, each 8'6" in length. Within each functional run, six active blocks (60" each) were interleaved with seven rest blocks (18" each). The active blocks consisted of one of the above noted videos, 3 of which were allocentric and 3 egocentric. Run order was randomized for each participant. Distinct stimuli were used during sessions 1 (List A) and 2 (List B) to avoid practice effects. Participants were instructed to press a button on an MRI-compatible response pad at the start of each block to ensure they were attending to the task. Task performance data from 2 HC and 1 MCI participants were lost due to equipment malfunction.

After completing the MRI portion of the study, participants were escorted to a quiet room where they completed a memory test using a touchscreen monitor and in-house software. For allocentric environments, participants were first shown a landmark (or key feature) and then shown a blank environment that contained a single landmark that was used to orient their cognitive map. They were instructed to touch the screen where they believed the target landmark belonged relative to the orienting landmark. Distance (in cm) between the actual and observed location was the primary outcome measure. For each egocentric environment, participants were shown an intersection and asked to touch either the left or right hallway, in consecutive order, thereby recalling the series of turns. The number of turns (in serial order) correctly recalled was the primary outcome measure.

HD-tDCS

HD-tDCS was performed in a quiet office ~30 feet from the MRI scanner. At the start of the session, study staff measured the participant's head and identified the site for the center anode (P2) and surrounding cathodes (CPz, CP6, POz, and PO8; Fig. 1b). Following our standard protocols, the team member created a cloth template using these measurements, which facilitated electrode placement during the second session. Surgilast head netting was then placed over the participant's head, HD

electrode holders (Soterix Medical Inc.) were positioned through the holes at the target locations, and the team member ensured the scalp was visible through the holder (e.g. by moving hair). Each holder was filled with ~10 mL conductive gel and checked to ensure there were no air bubbles. The silver/silver chloride HD electrode was then placed into the holder and additional gel added as necessary to ensure it was completely covered. The holder cap was then placed. As recently described (Hampstead et al. 2020), contact quality, as reflected by quality units (QUs), was measured at the start of the session as well as after a 10-min phase, the latter of which was designed to allow the gel to saturate the scalp and reduce impedance. Additional modifications (e.g. moving hair, adding gel) were made as necessary following these measurements with the goal of achieving a QU $\leq$ 2. After the 10-min saturation phase, the team member entered the participant and session specific code into the Clinical Trial unit (Soterix Medical, Inc.), which powered the attached 4×1 HD-tDCS unit (Soterix Medical, Inc.). A participant and session unique code was entered into the Clinical Trial unit at the start of each session, thereby ensuring both the study team and participant were blinded to the stimulation condition. Active stimulation was delivered at 2 mA for 20 min with a 30 s ramp up and ramp down period. Sham stimulation consisted of a 30 s ramp up to 2 mA followed immediately by 30 s ramp down at both the start and end of the session; an approach that capitalized on both primacy and recency of sensory side-effects. Participants completed a standard side-effect questionnaire (Brunoni et al. 2011; Reckow et al. 2018) and indicated whether they believed they received active or sham stimulation (As is generally the case, participants were unable to identify whether they received active or sham stimulation. Specifically, for active HD-tDCS, 29% of the participants believed it was active, 33% believed it was sham, and 38% were not sure. Likewise, for sham stimulation, 27% believed it was active, 29% believed it was sham, and 44% were not sure). Then, the electrodes and holders were removed, a vitamin E capsule placed at P2 and F5, and the participant immediately escorted to the MRI scanner.

MRI acquisition and preprocessing

Imaging data were collected using a 3 T General Electric MR750 scanner with a 32-channel head coil. First, resting-state data were acquired in interleaved ascending order using a gradient echo sequence, with MR parameters: TR/TE = 900/30 ms; multiband factor = 3; flip angle = 70°; field of view = 240 × 240 mm^2; matrix size = 74 × 74; slice thickness = 3 mm, no gap; 45 slices; voxel size = 3.24 × 3.24 × 3 mm^3. After an initial 5.4 s of signal stabilization, 506 volumes of resting-state were acquired. Then, task-related functional images were acquired in interleaved ascending order using a gradient echo sequence, with MR parameters: TR/TE = 1200/30 ms; multiband factor = 3;

flip angle = 70°; field of view = 220 × 220 mm^2; matrix size = 88 × 88; slice thickness = 2.5 mm, no gap; 51 slices; voxel size = 2.5 × 2.5 × 2.5 mm^3. After an initial 7.2 s of signal stabilization, 406 volumes of task data were acquired for each of the 3 runs. A high-resolution T_1-weighted anatomical image was also collected following resting-state and preceding task acquisition, using spoiled-gradient-recalled acquisition (SPGR) in steady-state imaging (TR/TE = 12.24/5.18 ms, flip angle = 15°, field of view = 256 × 256 mm^2, matrix size = 256 × 256; slice thickness = 1 mm; 156 slices; voxel size = 1 × 1 × 1 mm^3).

Preprocessing was performed using SPM12 (Wellcome Department of Cognitive Neurology, London) and MATLAB R2019b (The MathWorks Inc., Natick, MA). Functional images were slice-time corrected, realigned, and coregistered to the anatomical images in two steps, first within session and then to match the average anatomical image calculated across the two sessions. A study-specific anatomical template was created, using Diffeomorphic Anatomical Registration Through Exponentiated Lie Algebra (DARTEL) (Ashburner 2007), based on segmented gray matter and white matter tissue classes, to optimize inter-participant alignment (Klein et al. 2009). The DARTEL flowfields and MNI transformation were then applied to the functional images, and the functional images were resampled to 3 × 3 × 3 mm^3 voxel size. The average proportion of outlier scans (differential motion $d > 2$ mm or global intensity $z > 5$, identified with Artifact Detection Toolbox [ART]; ww.nitrc.org/projects/artifact_detect/) was < 3% in both HC (task: 1.66%, resting-state: 0.86%) and MCI (task: 2.32%, resting-state: 1.06%). There were no significant differences between HC and MCI participants in residual head motion (i.e. mean differential motion after accounting for outlier scans) or the amount of data retained (i.e. number of scans after accounting for outliers; all $ps > 0.1$; see Table 1).

Functional connectivity calculation

Brain-wide functional connectivity analyses were performed using the Connectivity Toolbox (CONN; Whitfield-Gabrieli and Nieto-Castanon 2012) and a commonly used functional atlas (Power et al. 2011). A 5 mm-radius sphere was centered at each atlas coordinate. We used 249 regions of interest (ROIs): 243 ROIs from the Power atlas that showed overlap with our functional data plus 6 additional regions identifying the anterior, mid, and posterior hippocampi. To remove physiological and other sources of noise from the fMRI time series, we used linear regression and the anatomical CompCor method (Behzadi et al. 2007; Chai et al. 2012; Muschelli et al. 2014). Each participant's white matter and cerebrospinal fluid masks derived during segmentation, eroded by 1 voxel to minimize partial volume effects, were used as noise ROIs. The following temporal covariates were added to the model: undesired linear trend, signal extracted from each participant's noise ROIs (5 principal component analysis parameters for each), motion parameters (3 rotation

and 3 translation parameters, plus their first-order temporal derivatives), regressors for each outlier scan (i.e. "scrubbing"; one covariate was added for each outlier scan, consisting of 0's everywhere but the outlier scan, coded as "1"). For the task-based functional connectivity analyses, to account for variance associated with task-related coactivation, additional task regressors, modeled as boxcar functions convolved with a canonical hemodynamic response function (HRF), were added for each condition as covariates of no interest. The residual fMRI time series were high-pass filtered (0.008 Hz). Functional connectivity was estimated using a Pearson's correlation between each pair of time series. For the task-related functional connectivity, the residual time series for each task block (accounting for hemodynamic delay by convolving the boxcar regressor for each block with a rectified HRF; Whitfield-Gabrieli and Nieto-Castanon 2012) were concatenated to form condition-specific time series for each brain region. Finally, the correlation coefficients were Fisher-z transformed, and the diagonal of the connectivity matrix was set to zero.

Electric field modeling and extraction

A realistic volumetric-approach to simulate transcranial electric stimulation (ROAST) was used to estimate the amount of electrical current *delivered* to each participant (Huang et al. 2019). The ROAST software segments each T_1 image in several tissue classes (e.g. gray matter, white matter), utilizes virtual electrodes at specified locations and current values to generate a finite element method mesh, and solves for electric field (EF) and voltage values across the entire brain. The tissue probability maps (TPM) within ROAST were replaced with the SPM12 default TPMs as this led to improved tissue class segmentation. For this study, one electrode montage was used for all participants, with electrode placements generated from ROAST. Specifically, the anode at P2 provided 2 mA of current while we assumed an equitable split (i.e. −0.5 mA) across the four cathodes (Fig. 1c). ROAST's default disc electrodes were used (6 mm radius, 2 mm height). The SPM canonical T1 head template was used to determine the location of the P2 electrode in MNI coordinates within ROAST. These coordinates were then converted into each subjects' space using an affine transformation, and a 10 mm-diameter sphere was built around these transformed coordinates. The intersection between the sphere and ROAST's segmentation of gray and white matter was defined as a ROI, and the average EF was extracted from each ROI (Fig. 1d and Table 1).

Segregation analyses

We computed network segregation (Chan et al. 2014; Wig 2017) using the Power et al. (2011) node-module assignments. Network segregation was defined as the difference of within- and between-network connectivity expressed as a proportion of within-network connectivity, i.e. $(\overline{Z}_w - \overline{Z}_b)/\overline{Z}_w$, where $\overline{Z}_w$ is the mean within-network connectivity and $\overline{Z}_b$ is the mean between-network

connectivity. Segregation analyses were performed at three levels of increasing granularity, namely whole-brain, system type, and individual network. First, for the whole-brain analysis, within- and between-network connectivity were averaged across all networks. Second, for the system-level analysis (Chan et al. 2014), within- and between-network connectivity were averaged separately for the association (i.e. cingulo-opercular, default-mode, dorsal attention, frontoparietal, salience, and ventral attention networks) and sensory-motor networks (i.e. auditory, somato-sensorimotor, and visual networks). (Here, by "system" we simply denote a set of functional networks.) Finally, for the network-level analysis, within-network connectivity was calculated for each individual network, whereas between-network connectivity was calculated for each individual network relative to all the other networks belonging to the same system (i.e. association or sensory-motor) and then averaged.

Segregation scores for each participant, condition, and session were exported to SPSS and analyzed within the ANOVA framework. Effect sizes are reported as partial eta squared (η_p^2). We examined the effects of HD-tDCS on functional connectivity using a Group (HC, MCI) × Order (Sham First, Active First) × Treatment (Sham, Active) × Task (Allocentric, Egocentric) mixed-effects ANOVA. Significant Group effects were followed-up with separate Order × Treatment × Task ANOVAs within each group.

Results
Behavioral results

Behavioral results showed better overall performance for HC relative to MCI patients, particularly for allocentric navigation, and no significant effects of HD-tDCS on performance for either allocentric or egocentric navigation. Specifically, for allocentric navigation, a Group×Order×Treatment ANOVA on recall error (i.e. distance [in cm] between the actual and observed location of each target landmark, averaged across presented environments) showed less error (i.e. better performance) for HC relative to MCI (M(SD) HC: 13.6 (0.52); MCI: 15.21 (0.52); $F_{1,34} = 4.77$, $P = 0.036$, $\eta_p^2 = 0.12$) and an unpredicted Order × Treatment interaction ($F_{1,34} = 8.56$, $P = 0.006$, $\eta_p^2 = 0.2$); there were no other significant effects ($ps > 0.3$; $\eta_p^2 < 0.02$). Similarly, for egocentric navigation, a Group × Order × Treatment ANOVA on recall error (i.e. number of turns in serial order correctly recalled) showed better performance for HC relative to MCI at a trend level (M(SD) HC: 9.41 (0.56); MCI: 7.88 (0.57); $F_{1,35} = 3.66$, $P = 0.064$, $\eta_p^2 = 0.1$), and no other significant effects ($ps > 0.1$; $\eta_p^2 < 0.05$).

Network segregation
Whole-brain network segregation

Whole-brain network segregation, computed by averaging the segregation values across all modules, is displayed in Figure 2. A Group × Order × Treatment
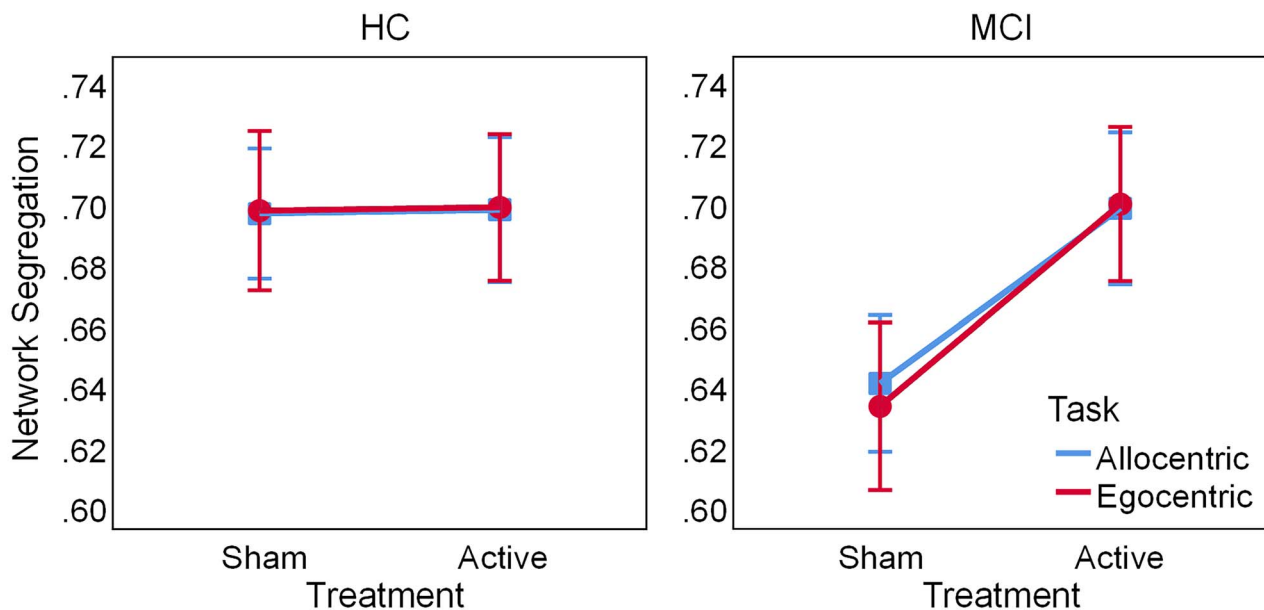
HC

MCI

Fig. 2. Whole-brain network segregation during spatial navigation. Active HD-tDCS increases segregation for MCI but not HC. Error bars display standard error of the mean. Abbreviations: HD-tDCS, high-definition transcranial direct current stimulation; HC, healthy controls; MCI, patients with mild cognitive impairment.

× Task ANOVA on task-related segregation showed a main effect of Treatment ($F_{1,38} = 7.53$, $P = 0.009$, $\eta_p^2 = 0.17$), qualified by a Group × Treatment interaction ($F_{1,38} = 6.99$, $P = 0.012$, $\eta_p^2 = 0.16$), and no other significant effects ($ps > 0.06$, $\eta_p^2 < 0.09$). Follow-up Order × Treatment × Task ANOVAs within each group confirmed that active HD-tDCS increased network segregation in MCI (Treatment: $F_{1,18} = 13.4$, $P = 0.002$, $\eta_p^2 = 0.43$) but not in HC (Treatment: $F_{1,20} = 0.005$, $P = 0.942$, $\eta_p^2 < 0.001$), relative to sham. Together, these results suggest that active HD-tDCS may normalize brain-wide network segregation during task performance in MCI. In addition, to check whether the effects of HD-tDCS would also be observed during resting-state, we performed a Group × Order × Treatment mixed-model ANOVA on resting-state brain-wide segregation; however, this analysis showed no significant effects ($ps > 0.2$, $\eta_p^2 < 0.03$; see Supplementary Results and Supplementary Fig. S1).

Segregation within sensory-motor and association systems

Segregation within the sensory-motor and association systems, calculated by averaging segregation values over the modules belonging to each system, is displayed in Figure 3. We performed separate Group × Order × Treatment × Task ANOVAs on task-related segregation within the sensory-motor and associative systems, respectively. First, within the sensory-motor system, there was a main effect of Task ($F_{1,38} = 30.05$, $P < 0.001$, $\eta_p^2 = 0.44$), indicating greater segregation between sensory-motor networks for allocentric compared to egocentric navigation; there was also an unpredicted Group × Order × Task interaction ($F_{1,38} = 5.91$, $P = 0.02$, $\eta_p^2 = 0.14$) and no other significant effects ($ps > 0.1$, $\eta_p^2 < 0.07$). Second, within the association system, there was a main effect of Treatment

($F_{1,38} = 8.66$, $P = 0.006$, $\eta_p^2 = 0.19$), qualified by a Group × Treatment interaction ($F_{1,38} = 8.48$, $P = 0.006$, $\eta_p^2 = 0.18$); there was also an unpredicted Group × Order interaction ($F_{1,38} = 7.6$, $P = 0.009$, $\eta_p^2 = 0.17$) and no other significant effects ($ps > 0.08$, $\eta_p^2 < 0.08$). Follow-up Order × Treatment × Task ANOVAs on network segregation within the association system, performed separately for each group, confirmed that active HD-tDCS increased segregation between the association networks for MCI patients (Treatment: $F_{1,18} = 11.64$, $P = 0.003$, $\eta_p^2 = 0.39$) but not for HC (Treatment: $F_{1,20} = 0.001$, $P = 0.977$, $\eta_p^2 < 0.001$), relative to sham. Of note, a Order × Treatment × Task × System ANOVA on within-system segregation for MCI patients yielded a medium/large effect for the Treatment × System interaction, although it did not reach significance ($F_{1,18} = 2.76$, $P = 0.11$, $\eta_p^2 = 0.13$), and we posit that this was likely due to lack of power for capturing an ordinal interaction, which is a known issue for ANOVA designs (see Bobko 1986; Strube and Bobko 1989). By comparison, the effect size of the Treatment × System interaction in a similar ANOVA for HC was virtually null ($F_{1,20} = 0.08$, $P = 0.786$, $\eta_p^2 = 0.004$). Together, these results suggest that, while the sensory-motor system is primarily responsive to the allocentric vs. egocentric nature of the navigation task, increased network segregation for active HD-tDCS in MCI is likely driven by changes within the association system.

Segregation of dorsal-attention, frontoparietal, and default-mode from other associative networks in MCI

Given the significant effects of active HD-tDCS on segregation within the association system only in MCI patients, we further examined the segregation between association networks within this group, focusing on three
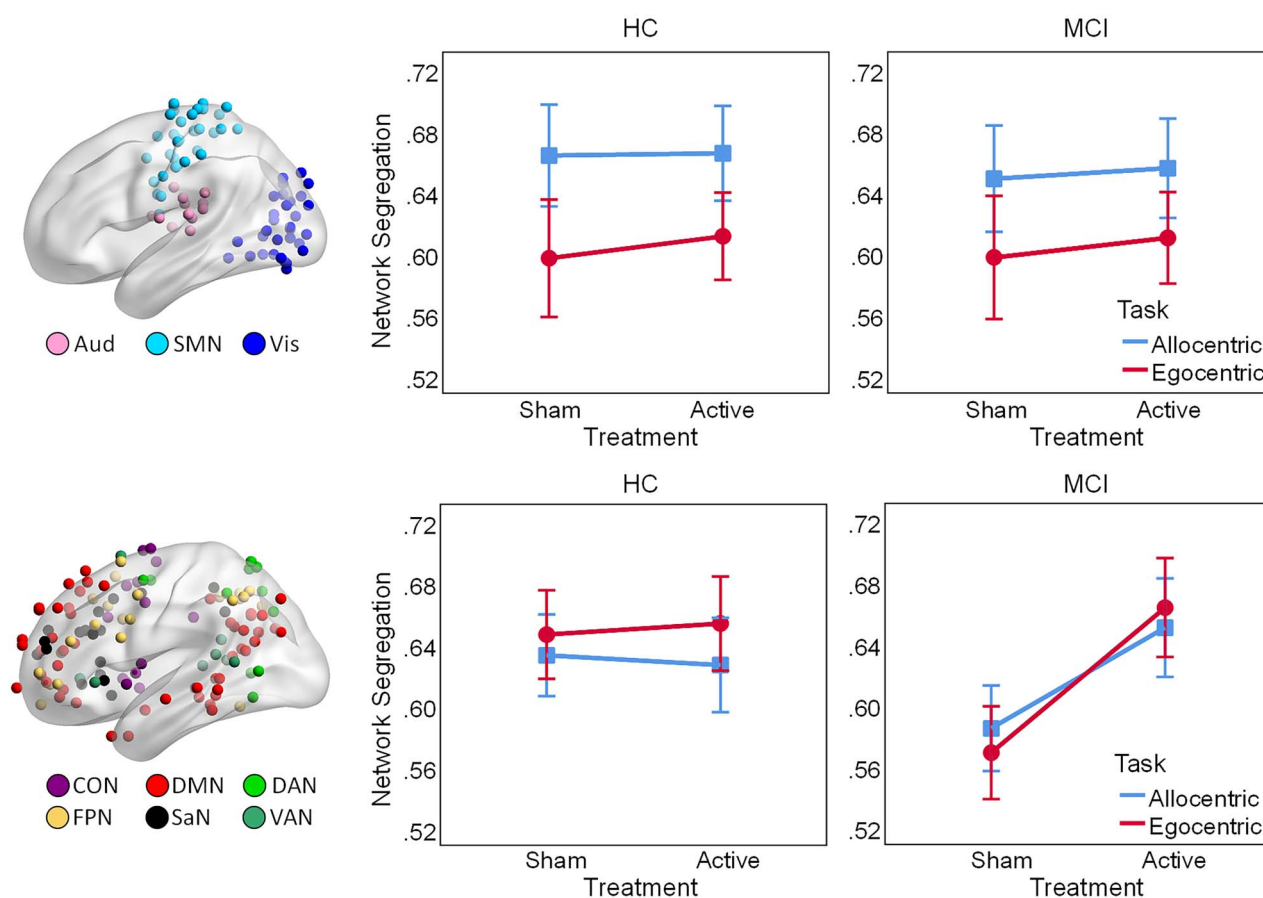
Fig. 3. Segregation within the sensory-motor (upper panel) and association systems (lower panel) during spatial navigation. Active HD-tDCS increases segregation within the association system in MCI. Colored spheres identify nodes of each network projected on the brain surface. Error bars display standard error of the mean. Abbreviations: Aud, auditory; SMN, somato-sensorimotor; Vis, visual; CON, cingulo-opercular; DMN, default-mode; DAN, dorsal-attention; FPN, frontoparietal; SaN, salience; VAN, ventral-attention network; HD-tDCS, high-definition transcranial direct current stimulation; HC, healthy controls; MCI, patients with mild cognitive impairment.

task-relevant networks that involve the targeted right parietal cortex, namely dorsal-attention, frontoparietal, and default-mode networks (Fig. 4). These analyses were justified by (1) our a priori hypotheses regarding the involvement of the three targeted networks (i.e. dorsal-attention, default-mode, and frontoparietal) and (2) significant Group × Treatment interactions on individual network segregation. Specifically, Group × Order × Treatment × Task ANOVAs on network segregation yielded significant Group × Treatment interactions for the dorsal-attention ($F_{1,38} = 9.39$, $P = 0.004$, $\eta_p^2 = 0.2$) and default-mode networks ($F_{1,38} = 5.73$, $P = 0.022$, $\eta_p^2 = 0.13$), whereas the Group × Treatment interaction for the frontoparietal network was only a trend ($F_{1,38} = 3.64$, $P = 0.064$, $\eta_p^2 = 0.09$). Further exploratory analyses (see Supplementary Results) also identified a trending Group × Treatment interaction for salience ($F_{1,38} = 3.51$, $P = 0.069$, $\eta_p^2 = 0.09$) but not for any other association (or sensory-motor) networks ($ps > 0.1$, $\eta_p^2 < 0.05$).

As planned, we performed Order × Treatment × Task ANOVAs on task-related segregation of the dorsal-attention, frontoparietal, and default-mode networks, respectively. First, regarding the dorsal-attention network, there was greater segregation following active compared to sham stimulation (Treatment: $F_{1,18} = 13.47$, $P = 0.002$, $\eta_p^2 = 0.43$) and greater segregation for allocentric compared to egocentric navigation (Task: $F_{1,18} = 36.43$, $P < 0.001$, $\eta_p^2 = 0.67$), indicating additive effects of HD-tDCS and task on dorsal-attention network segregation; there were no other significant effects ($ps > 0.1$, $\eta_p^2 < 0.14$). Second, regarding the frontoparietal network, there was a main effect of Task ($F_{1,18} = 10.24$, $P = 0.005$, $\eta_p^2 = 0.36$) and a trend for Treatment × Task interaction ($F_{1,18} = 3.79$, $P = 0.067$, $\eta_p^2 = 0.17$), indicating greater frontoparietal network segregation following active HD-tDCS for the egocentric compared to the allocentric task. Finally, regarding the default-mode network, there were additive effects of Treatment and Task, with greater segregation following active compared to sham stimulation (Treatment: $F_{1,18} = 8.69$, $P = 0.009$, $\eta_p^2 = 0.33$) and greater segregation for egocentric compared to allocentric navigation (Task: $F_{1,18} = 13.06$, $P = 0.002$, $\eta_p^2 = 0.42$); there was also an unpredicted main effect of Order ($F_{1,18} = 4.61$, $P = 0.046$, $\eta_p^2 = 0.2$) and no other significant effects ($ps > 0.07$, $\eta_p^2 < 0.17$). Exploratory analyses on within- and between-network connectivity suggest that greater network segregation following active HD-tDCS in MCI patients may be primarily driven by
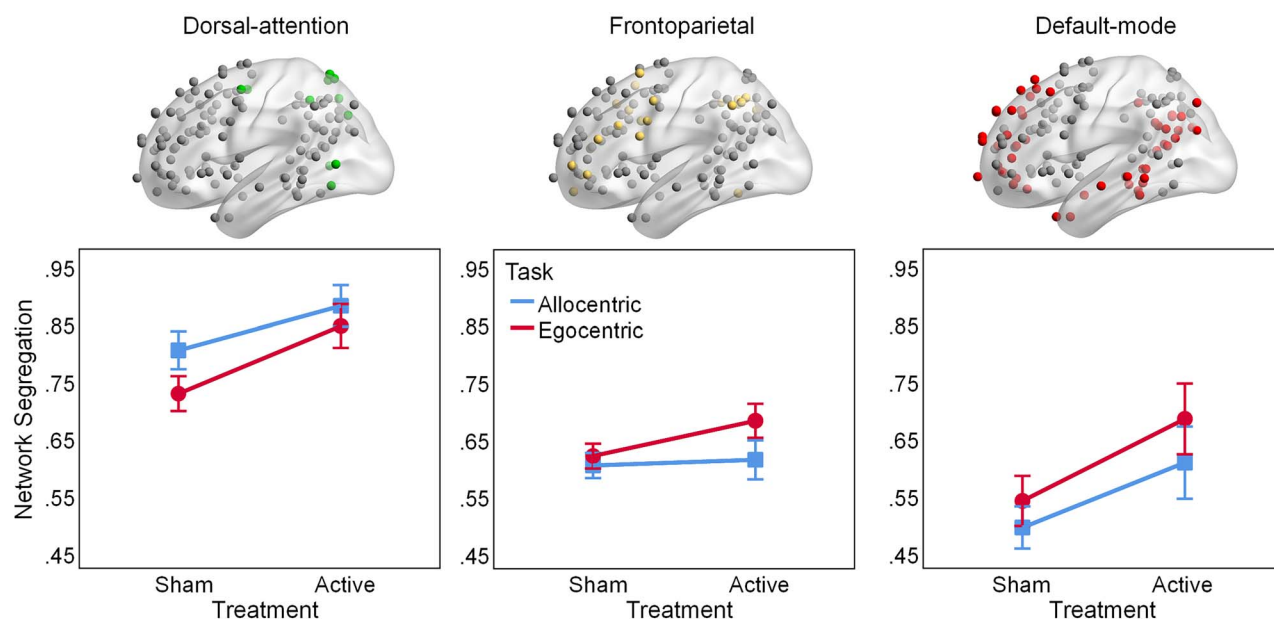
Fig. 4. Segregation of dorsal-attention, frontoparietal, and default-mode networks from other association networks, during spatial navigation, for MCI patients. Active HD-tDCS increases segregation of dorsal-attention and default-mode networks from other association networks in MCI. Error bars display standard error of the mean. Abbreviations: HD-tDCS, high-definition transcranial direct current stimulation; MCI, patients with mild cognitive impairment.

reductions of between-network connectivity among the association networks (see Supplementary Results and Supplementary Fig. S2). In sum, results suggest that HD-tDCS effects for MCI patients were primarily driven by the dorsal-attention and default-mode networks, consistent with their complementary roles in processing oriented toward the external and internal environments, respectively.

Discussion

The present study identified both lower overall navigation performance and lower baseline (i.e. following sham HD-tDCS) network segregation in MCI patients compared to HC, consistent with prior work (Brier et al. 2014; Damoiseaux 2017). In addition, we showed that the difference in brain-wide network segregation between MCI patients and HC was primarily driven by the association networks, whereas the sensory-motor networks were more sensitive to the allocentric versus egocentric nature of the task. Critically, segregation of the associative networks increased following active HD-tDCS only for MCI patients and achieved levels similar to HC. This suggests that HD-tDCS (center anode) may *normalize* network segregation in MCI patients; however, no changes were detected at the level of behavioral performance, suggesting that "dose" effects are critical (discussed below). At the same time, the lack of HD-tDCS effects in HC may be due to this group already showing optimal network segregation during task performance. Indeed, higher performance on specialized tasks has been associated with greater network segregation (Bassett et al. 2011;

Finc et al. 2020). Of note, the effects of HD-tDCS on segregation were specific for task performance, as no HD-tDCS effects were observed during resting-state for either MCI patients or HC. This suggests that the functional state of the targeted brain regions/networks influences the effects of tDCS, in line with the "functional targeting" hypothesis (Guleyupoglu et al. 2013).

At the level of brain systems, our results showed increased segregation following HD-tDCS within the association system, but not within the sensory-motor system, and only for the MCI patients. This suggests that the normalization of whole-brain segregation for MCI patients was driven by stimulation-related effects within the association system. In contrast, segregation within the sensory-motor system was influenced only by the nature of the task, with both groups showing greater segregation during allocentric than egocentric navigation. This suggests that the sensory-motor networks may be more selectively recruited during allocentric navigation, consistent with prior evidence (Hampstead et al. 2014).

Follow-up analyses in MCI patients at the level of individual networks showed that HD-tDCS increased segregation of the dorsal-attention and default-mode networks from the other associative networks. Together with the results outlined above, this suggests that normalization of segregation for MCI patients was driven by modulation of the dorsal-attention and default-mode networks for both brain-wide and association system analyses. In addition, there was a subtask specific effect independent of HD-tDCS, where the dorsal-attention network showed greater segregation from the other association networks during allocentric navigation, whereas the default-mode network showed greater segregation

during egocentric navigation. This is consistent with the putatively distinct specializations of these two networks, namely processing oriented toward the external environment (dorsal-attention—i.e. attending to landmarks and spatial relationships) vs. the internal environment (default-mode—i.e. attending to self-referential relationships of left vs. right turns) (Fox et al. 2005; Spreng et al. 2013; Dixon et al. 2017). Finally, only the frontoparietal network showed a trending Treatment × Task interaction indicating greater tDCS-related reorganization during egocentric than allocentric navigation, a pattern more similar to the default-mode than the dorsal-attention network. Given the task-dependent fractionation of the frontoparietal network (Dixon et al. 2018), this may reflect greater HD-tDCS impact on the frontoparietal component preferentially involved in the regulation of introspective processes.

Limitations and future directions

Despite the observed neurophysiological effects at the level of brain networks, neither group showed altered memory test performance. We suspect this reflects an insufficient "dose" of HD-tDCS which could be conceptualized as either (or both) the amount of current delivered to the brain or the number of sessions provided. Regarding the former, the individualized models demonstrated two critical findings. First, there was marked variability in the amount of current delivered, on the order of 370% (range [0.07, 0.31] V/m), which raises the possibility that some participants simply did not receive enough stimulation to evidence an effect. Second, the models revealed a small overall amount of delivered current reached the brain region, as reflected by the peak of 0.31 V/m, which is below known dose–response curves (Esmaeilpour et al. 2018). While sufficient to restore a relatively fragile network in those with MCI, the EF may have been insufficient to affect the HC group. Of note, correlations between network segregation and behavioral performance, as well as correlations linking the amount of current delivered with segregation and behavioral performance, were not significant (all $ps > 0.1$). These null results may be due to the relatively small samples (Schönbrodt and Perugini 2013), and future studies, with larger samples, are needed to investigate these aspects further. Another potential source of variability may be represented by variations in the location of peak stimulation across participants (e.g. Indahlastari et al. 2019; Indahlastari et al. 2020). In addition to the limited magnitude and range of delivered stimulation, we selected EF values from only a single location (under P2), which is a reasonable approach but likely fails to capture the overall "dose" delivered to all affected regions. We are currently developing methods to better account for the presence/absence and magnitude of delivered current in individual regions, which may clarify such dose–response relationships in the future.

Regarding the number of sessions, it is likely unreasonable to expect that a single session would enhance cognitive performance in a population that has experienced progressive change as a function of "normal" aging (i.e. controls), let alone in one with additional superimposed disease-related change (i.e. the MCI group). The network level changes are critical in this regard since they demonstrate that HD-tDCS "restored" network functioning and raise the possibility that, with sustained efforts (e.g. multiple sessions), cognition would also improve. These findings form the basis for our ongoing randomized controlled trial of dose–response relationships in those with MCI and dementia of the Alzheimer's type (NCT03875326).

Another potential limitation of our study is that there were no fMRI data collected prior to participant randomization. However, because we *directly* compared active versus sham HD-tDCS, our design controlled for any nonspecific effects associated with setting-up the HD-tDCS montage or potential sensory experiences (i.e. tingling) associated with the initial ramp-up and final ramp-down of the stimulation. Therefore, sham HD-tDCS constituted a much stricter control for active HD-tDCS than a prerandomization baseline. While the number of days between sessions had no significant effects on navigation performance (see Supplementary Results), future studies should explicitly address potential order effects and better define wash-out periods.

Conclusions

In sum, we provide initial fMRI evidence for restorative effects of HD-tDCS on task-related functional network organization in MCI patients. The balance between network segregation and integration is critical for efficient brain function, but is already affected in preclinical AD (Brier et al. 2014). Our results show that, while network segregation during spatial navigation is normally lower in MCI patients compared to HC, HD-tDCS over the right parietal cortex may be able to restore it to levels observed in HC. The present findings advance our understanding of the effects of brain stimulation on functional network organization in MCI and open new avenues for applying (HD-) tDCS as a targeted system-level intervention for restoring brain activity in AD and related dementias. Additional work will be needed to establish the parameters necessary to translate such system-level changes into meaningful and sustained real-world behavioral change.

Acknowledgments

Supplementary material

Supplementary material is available at *Cerebral Cortex* online.

Funding

Data Availability Statement

The data sets analyzed for this study may be available upon request to the corresponding author, pending approval from participants and adherence with the Department of Veterans Affairs central and local approval mechanisms.

References

Albert MS, DeKosky ST, Dickson D, Dubois B, Feldman HH, Fox NC, Gamst A, Holtzman DM, Jagust WJ, Petersen RC, et al. The diagnosis of mild cognitive impairment due to Alzheimer's disease: recommendations from the national institute on aging-Alzheimer's association workgroups on diagnostic guidelines for Alzheimer's disease. *Alzheimers Dement*. 2011:7:270–279.

Ashburner J. A fast diffeomorphic image registration algorithm. *NeuroImage*. 2007:38:95–113.

Bassett DS, Wymbs NF, Porter MA, Mucha PJ, Carlson JM, Grafton ST. Dynamic reconfiguration of human brain networks during learning. *Proc Natl Acad Sci U S A*. 2011:108:7641–7646.

Behzadi Y, Restom K, Liau J, Liu TT. A component based noise correction method (compcor) for bold and perfusion based fMRI. *NeuroImage*. 2007:37:90–101.

Bobko P. A solution to some dilemmas when testing hypotheses about ordinal interactions. *J Appl Psychol*. 1986:71:323–326.

Boccia M, Nemmi F, Guariglia C. Neuropsychology of environmental navigation in humans: review and meta-analysis of fMRI studies in healthy participants. *Neuropsychol Rev*. 2014:24:236–251.

Brier MR, Thomas JB, Fagan AM, Hassenstab J, Holtzman DM, Benzinger TL, Morris JC, Ances BM. Functional connectivity and graph theory in preclinical Alzheimer's disease. *Neurobiol Aging*. 2014:35:757–768.

Brunoni AR, Amadera J, Berbel B, Volz MS, Rizzerio BG, Fregni F. A systematic review on reporting and assessment of adverse effects associated with transcranial direct current stimulation. *Int J Neuropsychopharmacol*. 2011:14:1133–1145.

Brunyé TT. Modulating spatial processes and navigation via transcranial electrical stimulation: a mini review. *Front Hum Neurosci*. 2017:11:649.

Buckner RL, Andrews-Hanna JR, Schacter DL. The brain's default network: anatomy, function, and relevance to disease. *Ann N Y Acad Sci*. 2008:1124:1–38.

Cano T, Morales-Quezada JL, Bikson M, Fregni F. Methods to focalize noninvasive electrical brain stimulation: principles and future clinical development for the treatment of pain. *Expert Rev Neurother*. 2013:13:465–467.

Chai XJ, Castanon AN, Ongur D, Whitfield-Gabrieli S. Anticorrelations in resting state networks without global signal regression. *NeuroImage*. 2012:59:1420–1428.

Chan MY, Park DC, Savalia NK, Petersen SE, Wig GS. Decreased segregation of brain systems across the healthy adult lifespan. *Proc Natl Acad Sci U S A*. 2014:111:E4997–E5006.

Cona G, Scarpazza C. Where is the "where" in the brain? A meta-analysis of neuroimaging studies on spatial cognition. *Hum Brain Mapp*. 2019:40:1867–1886.

Corbetta M, Shulman GL. Control of goal-directed and stimulus-driven attention in the brain. *Nat Rev Neurosci*. 2002:3:201–215.

Crossley NA, Mechelli A, Vertes PE, Winton-Brown TT, Patel AX, Ginestet CE, McGuire P, Bullmore ET. Cognitive relevance of the community structure of the human brain functional coactivation network. *Proc Natl Acad Sci U S A*. 2013:110:11583–11588.

Damoiseaux JS. Effects of aging on functional and structural brain connectivity. *NeuroImage*. 2017:160:32–40.

Dehaene S, Kerszberg M, Changeux JP. A neuronal model of a global workspace in effortful cognitive tasks. *Proc Natl Acad Sci U S A*. 1998:95:14529–14534.

Dixon ML, Andrews-Hanna JR, Spreng RN, Irving ZC, Mills C, Girn M, Christoff K. Interactions between the default network and dorsal attention network vary across default subsystems, time, and cognitive states. *NeuroImage*. 2017:147:632–649.

Dixon ML, De La Vega A, Mills C, Andrews-Hanna J, Spreng RN, Cole MW, Christoff K. Heterogeneity within the frontoparietal control network and its relationship to the default and dorsal attention networks. *Proc Natl Acad Sci U S A*. 2018:115:E1598–e1607.

Dosenbach NU, Fair DA, Miezin FM, Cohen AL, Wenger KK, Dosenbach RA, Fox MD, Snyder AZ, Vincent JL, Raichle ME, et al. Distinct brain networks for adaptive and stable task control in humans. *Proc Natl Acad Sci U S A*. 2007:104:11073–11078.

Duncan J. The multiple-demand (md) system of the primate brain: mental programs for intelligent behaviour. *Trends Cogn Sci*. 2010:14:172–179.

Ekstrom AD, Huffman DJ, Starrett M. Interacting networks of brain regions underlie human spatial navigation: a review and novel synthesis of the literature. *J Neurophysiol*. 2017:118: 3328–3344.

Esmaeilpour Z, Marangolo P, Hampstead BM, Bestmann S, Galletta E, Knotkova H, Bikson M. Incomplete evidence that increasing current intensity of TDCS boosts outcomes. *Brain Stimul*. 2018:11: 310–321.

Finc K, Bonna K, He X, Lydon-Staley DM, Kühn S, Duch W, Bassett DS. Dynamic reconfiguration of functional brain networks during working memory training. *Nat Commun*. 2020:11:2435.

Fox MD, Snyder AZ, Vincent JL, Corbetta M, Van Essen DC, Raichle ME. The human brain is intrinsically organized into dynamic, anticorrelated functional networks. *Proc Natl Acad Sci U S A*. 2005:102:9673–9678.

Geerligs L, Renken RJ, Saliasi E, Maurits NM, Lorist MM. A brain-wide study of age-related changes in functional connectivity. *Cereb Cortex*. 2015:25:1987–1999.

Grady C. The cognitive neuroscience of ageing. *Nat Rev Neurosci*. 2012:13:491–505.

Greicius MD, Krasnow B, Reiss AL, Menon V. Functional connectivity in the resting brain: a network analysis of the default mode hypothesis. *Proc Natl Acad Sci U S A*. 2003:100:253–258.

Guleyupoglu B, Schestatsky P, Edwards D, Fregni F, Bikson M. Classification of methods in transcranial electrical stimulation (TES) and

evolving strategy from historical approaches to contemporary innovations. *J Neurosci Methods*. 2013:219:297–311.

Hampstead BM, Brown GS, Hartley JF. Transcranial direct current stimulation modulates activation and effective connectivity during spatial navigation. *Brain Stimul*. 2014:7:314–324.

Hampstead BM, Ehmann M, Rahman-Filipiak A. Reliable use of silver chloride HD-TDCS electrodes. *Brain Stimul*. 2020:13:1005–1007.

Huang Y, Datta A, Bikson M, Parra LC. Realistic volumetric-approach to simulate transcranial electric stimulation-roast-a fully automated open-source pipeline. *J Neural Eng*. 2019:16:056006.

Indahlastari A, Albizu A, Nissim NR, Traeger KR, O'Shea A, Woods AJ. Methods to monitor accurate and consistent electrode placements in conventional transcranial electrical stimulation. *Brain Stimul*. 2019:12:267–274.

Indahlastari A, Albizu A, O'Shea A, Forbes MA, Nissim NR, Kraft JN, Evangelista ND, Hausman HK, Woods AJ. Modeling transcranial electrical stimulation in the aging brain. *Brain Stimul*. 2020:13: 664–674.

Iordan AD, Cooke KA, Moored KD, Katz B, Buschkuehl M, Jaeggi SM, Jonides J, Peltier SJ, Polk TA, Reuter-Lorenz PA. Aging and network properties: stability over time and links with learning during working memory training. *Front Aging Neurosci*. 2018:9:419.

Jerde TA, Curtis CE. Maps of space in human frontoparietal cortex. *J Physiol Paris*. 2013:107:510–516.

Keeser D, Meindl T, Bor J, Palm U, Pogarell O, Mulert C, Brunelin J, Möller HJ, Reiser M, Padberg F. Prefrontal transcranial direct current stimulation changes connectivity of resting-state networks during fMRI. *J Neurosci*. 2011:31:15284–15293.

Klein A, Andersson J, Ardekani BA, Ashburner J, Avants B, Chiang MC, Christensen GE, Collins DL, Gee J, Hellier P, et al. Evaluation of 14 nonlinear deformation algorithms applied to human brain MRI registration. *NeuroImage*. 2009:46:786–802.

Krishnamurthy V, Gopinath K, Brown GS, Hampstead BM. Resting-state fMRI reveals enhanced functional connectivity in spatial navigation networks after transcranial direct current stimulation. *Neurosci Lett*. 2015:604:80–85.

Kuo HI, Bikson M, Datta A, Minhas P, Paulus W, Kuo MF, Nitsche MA. Comparing cortical plasticity induced by conventional and high-definition 4 × 1 ring TDCS: a neurophysiological study. *Brain Stimul*. 2013:6:644–648.

Lebedev AV, Nilsson J, Lovden M. Working memory and reasoning benefit from different modes of large-scale brain dynamics in healthy older adults. *J Cogn Neurosci*. 2018:30:1033–1046.

Li LM, Violante IR, Leech R, Ross E, Hampshire A, Opitz A, Rothwell JC, Carmichael DW, Sharp DJ. Brain state and polarity dependent modulation of brain networks by transcranial direct current stimulation. *Hum Brain Mapp*. 2019:40:904–915.

Meinzer M, Lindenberg R, Phan MT, Ulm L, Volk C, Flöel A. Transcranial direct current stimulation in mild cognitive impairment: Behavioral effects and neural mechanisms. *Alzheimers Dement*. 2015:11:1032–1040.

Muschelli J, Nebel MB, Caffo BS, Barber AD, Pekar JJ, Mostofsky SH. Reduction of motion-related artifacts in resting state fMRI using aCompCor. *NeuroImage*. 2014:96:22–35.

Park DC, Polk TA, Park R, Minear M, Savage A, Smith MR. Aging reduces neural specialization in ventral visual cortex. *Proc Natl Acad Sci U S A*. 2004:101:13091–13095.

Peña-Gómez C, Sala-Lonch R, Junqué C, Clemente IC, Vidal D, Bargalló N, Falcón C, Valls-Solé J, Pascual-Leone Á, Bartrés-Faz D. Modulation of large-scale brain networks by transcranial direct current stimulation evidenced by resting-state functional MRI. *Brain Stimul*. 2012:5:252–263.

Petersen RC. Mild cognitive impairment: transition from aging to Alzheimer's disease. In: Iqbal K, Sisodia SS, Winblad B, editors. *Alzheimer's disease: advances in etiology, pathogenesis and therapeutics*. New York: Wiley; 2001. pp. 141–151

Petersen SE, Posner MI. The attention system of the human brain: 20 years after. *Annu Rev Neurosci*. 2012:35:73–89.

Petersen RC, Roberts RO, Knopman DS, Boeve BF, Geda YE, Ivnik RJ, Smith GE, Jack CR Jr. Mild cognitive impairment: ten years later. *Arch Neurol*. 2009:66:1447–1455.

Polanía R, Nitsche MA, Paulus W. Modulating functional connectivity patterns and topological functional organization of the human brain with transcranial direct current stimulation. *Hum Brain Mapp*. 2011:32:1236–1249.

Power JD, Petersen SE. Control-related systems in the human brain. *Curr Opin Neurobiol*. 2013:23:223–228.

Power JD, Cohen AL, Nelson SM, Wig GS, Barnes KA, Church JA, Vogel AC, Laumann TO, Miezin FM, Schlaggar BL, et al. Functional network organization of the human brain. *Neuron*. 2011:72: 665–678.

Raichle ME, MacLeod AM, Snyder AZ, Powers WJ, Gusnard DA, Shulman GL. A default mode of brain function. *Proc Natl Acad Sci U S A*. 2001:98:676–682.

Reckow J, Rahman-Filipiak A, Garcia S, Schlaefflin S, Calhoun O, DaSilva AF, Bikson M, Hampstead BM. Tolerability and blinding of 4x1 high-definition transcranial direct current stimulation (HD-TDCS) at two and three milliamps. *Brain Stimul*. 2018:11:991–997.

Sale MV, Mattingley JB, Zalesky A, Cocchi L. Imaging human brain networks to improve the clinical efficacy of non-invasive brain stimulation. *Neurosci Biobehav Rev*. 2015:57:187–198.

Schönbrodt FD, Perugini M. At what sample size do correlations stabilize? *J Res Pers*. 2013:47:609–612.

Sehm B, Kipping J, Schäfer A, Villringer A, Ragert P. A comparison between uni- and bilateral TDCS effects on functional connectivity of the human motor cortex. *Front Hum Neurosci*. 2013:7:183.

Smallwood J, Bernhardt BC, Leech R, Bzdok D, Jefferies E, Margulies DS. The default mode network in cognition: a topographical perspective. *Nat Rev Neurosci*. 2021:22:503–513

Spreng RN, Sepulcre J, Turner GR, Stevens WD, Schacter DL. Intrinsic architecture underlying the relations among the default, dorsal attention, and frontoparietal control networks of the human brain. *J Cogn Neurosci*. 2013:25:74–86.

Strube MJ, Bobko P. Testing hypotheses about ordinal interactions: simulations and further comments. *J Appl Psychol*. 1989:74: 247–252.

To WT, De Ridder D, Hart J Jr, Vanneste S. Changing brain networks through non-invasive neuromodulation. *Front Hum Neurosci*. 2018:12:128.

Whitfield-Gabrieli S, Nieto-Castanon A. Conn: a functional connectivity toolbox for correlated and anticorrelated brain networks. *Brain Connect*. 2012:2:125–141.

Wig GS. Segregated systems of human brain networks. *Trends Cogn Sci*. 2017:21:981–996.